0026-895X/04/6605-1147–1159$20.00
MOLECULAR PHARMACOLOGY
Copyright © 2004 The American Society for Pharmacology and Experimental Therapeutics
Mol Pharmacol 66:1147–1159, 2004

Vol. 66, No. 5
1107/1179095
Printed in U.S.A.

Specific Inhibition of Nuclear Factor-κB–Dependent Inflammatory Responses by Cell Type-Specific Mechanisms upon A_{2A} Adenosine Receptor Gene Transfer

William A. Sands, Anthony F. Martin, Elaine W. Strong, and Timothy M. Palmer

Molecular Pharmacology Group, Division of Biochemistry and Molecular Biology, Institute of Biomedical and Life Sciences, University of Glasgow, Glasgow, Scotland, United Kingdom

Received April 6, 2004; accepted July 30, 2004

ABSTRACT

Adenosine is a potent inhibitor of inflammatory processes, and the A_{2A} adenosine receptor (A_{2A}AR) plays a key nonredundant role as a suppresser of inflammatory responses in vivo. In this study, we demonstrate that increasing A_{2A}AR gene expression suppressed multiple inflammatory responses in both human umbilical vein endothelial cells (HUVECs) and rat C6 glioma cells in vitro. In particular, the induction of the adhesion molecule E-selectin by either tumor necrosis factor α (TNFα) or *Escherichia coli* lipopolysaccharide (LPS) was reduced by more than 70% in HUVECs, whereas inducible nitric-oxide synthase (iNOS) induction was abolished in C6 cells after exposure to interferon-γ in combination with LPS and TNFα, suggesting that the receptor inhibited a common step in the induction of each of these pro-inflammatory genes. Consistent with this hypothesis, A_{2A}AR expression inhibited the activation of NF-κB, a key transcription factor whose proper function was essential for optimal iNOS and E-selectin induction. However, although NF-κB binding to target DNA was severely compromised in both cell types, the mechanisms by which this occurred were distinct. In C6 cells, A_{2A}AR expression blocked IκBα degradation by inhibiting stimulus-induced phosphorylation, whereas in HUVECs, A_{2A}AR expression inhibited NF-κB translocation to the nucleus independently of any effect on IκBα degradation. Together, these observations suggest that A_{2A}AR-mediated inhibition NF-κB activation is a critical aspect of its anti-inflammatory signaling properties and that the molecular basis of this inhibition varies in a cell type-specific manner.

Extracellular levels of the ubiquitous nucleoside adenosine are a critical regulator of cardiovascular and central nervous system homeostasis. Upon its extracellular accumulation after metabolic stress, adenosine exerts a plethora of protective effects on target tissues that are mediated by its binding to four types of cell surface G-protein-coupled adenosine receptor (AR) proteins, termed A_1, A_{2A}, A_{2B}, and A_3 (Fredholm et al., 2001; Linden, 2001). It is noteworthy that several inflammatory cell types have been shown to be particularly responsive to the adenosine released during hypoxia, including neutrophils, endothelial cells (ECs), and glial cells (Banerjee et al., 2002; Sitkovsky et al., 2004). From these studies, the A_{2A}AR signaling system has emerged as a key pathway by which excessive inflammatory responses can be attenuated. For example, phorbol ester-mediated increases in neutrophil adhesion to ECs isolated from porcine aorta can be inhibited by prior treatment of ECs with A_{2A}AR agonists NECA and CGS21680 but not by the A_1AR-selective agonist N^6-cyclopentyladenosine (CPA) (Felsch et al., 1995). Second, exposure of human umbilical vein ECs (HUVECs) to exogenous adenosine partially reduces TNFα-stimulated leukocyte adhesion by inhibiting the induction of vascular cell adhesion molecule-1 and E-selectin, two critical adhesion molecules

This work was supported by project grants from the British Heart Foundation and National Heart Research Fund, equipment grants from Tenovus-Scotland and The Wellcome Trust (to T.M.P.) and studentships from the Medical Research Council (to A.F.M.) and British Heart Foundation (to E.W.S.).
Article, publication date, and citation information can be found at http://molpharm.aspetjournals.org.
doi:10.1124/mol.104.001107.

ABBREVIATIONS: AR, adenosine receptor; EC, endothelial cell; NECA, 5′-*N*-ethylcarboxamidoadenosine; CGS21680, 2-(*p*-carboxyethyl)phenylamino-5′-*N*-ethylcarboxamidoadenosine; CPA, N^6-cyclopentyladenosine; HUVEC, human umbilical vein endothelial cell; TNFα, tumor necrosis factor α; iNOS, inducible nitric-oxide synthase; NF-κB, nuclear factor κB; LPS, lipopolysaccharide; IFN, interferon; AV, adenovirus; WT, wild type; GFP, green fluorescent protein; m.o.i., multiplicity of infection; DTT, dithiothreitol; pfu, plaque-forming units; PBS, phosphate-buffered saline; BSA, bovine serum albumin; JNK, c-Jun N-terminal kinase; PMSF, phenylmethylsulfonyl fluoride; GST, glutathione *S*-transferase; PBSGG, phosphate-buffered saline/goat serum/gelatin; ZM241385, 4-(2-[7-amino-2-{2-furyl}{1,2,4}triazolo{2,3-*a*}{1,3,5}triazin-5-yl-amino]ethyl)phenol; PDTC, pyrrolidine dithiocarbamate; NAcCys, *N*-acetylcysteine; IKK, IκB kinase; PD, positive regulatory domain; SB203580, 4-(4-fluorophenyl)-2-(4-methylsulfinylphenyl)-5-(4-pyridyl)1*H*-imidazole; TLR, Toll-like receptor; ELISA, enzyme-linked immunosorbent assay.

that mediate EC-leukocyte interaction, and also by inhibiting the induction of at least two pro-inflammatory cytokines, interleukins 1 and 6 (Bouma et al., 1996). Third, the nonsteroidal anti-inflammatory drugs sulfasalazine and methotrexate exert their anti-inflammatory effects by promoting ecto-5′-nucleotidase-mediated conversion of adenine nucleotides to adenosine. The resulting elevated levels of adenosine can then act upon endogenous A_{2A} and A_3ARs on ECs and neutrophils to inhibit inflammatory responses (Cronstein et al., 1999; Montesinos et al., 2000). Finally, the importance of the A_{2A}AR as a constitutive repressor of inflammatory responses in vivo has been demonstrated by the enhanced responses to bacterial endotoxin observed in mice in which the A_{2A}AR gene has been deleted (Ohta and Sitkovsky, 2001).

However, despite numerous observations describing the anti-inflammatory effects of A_{2A}AR activation in a variety of cellular systems, relatively little is known about the molecular mechanisms by which they occur. In this study, we demonstrate that elevating A_{2A}AR protein expression in glioma cells and vascular ECs is sufficient to markedly inhibit inflammatory responses to maximally effective concentrations of pro-inflammatory stimuli. In addition, we demonstrate that the receptor can exert these effects by specifically blocking activation of the critical transcription factor NF-κB via distinct cell type-specific mechanisms.

Materials and Methods

Materials. The human A_{2A}AR gene was generously donated by Dr. Andrea Townsend-Nicholson (Royal Free Hospital, London, U.K.). GeneJuice transfection reagent was from Novagen (Madison, WI). HUVECs plus appropriate growth medium and supplements were from Cambrex Bio Science Nottingham Ltd. (Nottingham, UK). Nucleofection reagents were from Amaxa (Cologne, Germany). Antibodies were obtained from Santa Cruz Biotechnology (Santa Cruz, CA) (IκBα, RelA/p65, 12CA5), Serotec (Oxford, UK) (E-selectin monoclonal antibody 1.2B6), BD Biosciences (Palo Alto, CA) [inducible nitric-oxide synthase (iNOS)], and Cell Signaling Technology Inc. (Beverly, MA) ($Ser^{32}Ser^{36}$-phosphorylated IκBα, Ser^{63}-phosphorylated c-jun, and $Thr^{180}Tyr^{182}$-phosphorylated and total p38). The NF-κB oligonucleotide probe was from Santa Cruz Biotechnology. *Escherichia coli* 0111:B4 LPS, rat and human TNFα, and rat interferon-γ (IFNγ) were from Sigma-Aldrich. A 3-κB enhancer conA-luciferase reporter plasmid, sheep nonimmune antobodies, and anti-p50 and -p65 antibodies used for supershift experiments were generously donated by Prof. Ron Hay (University of St. Andrews, UK). A control pSV-β-galactosidase expression construct was from Promega. A bacterial expression plasmid that directed expression of GST-c-jun(1–79) and rabbit anti-JNK1,2 polyclonal antibody were generously donated by Prof. David Gillespie (Cancer Research UK Beatson Laboratories, Glasgow, UK). A control adenovirus (AV) that directed the expression of GFP alone, termed AV/GFP, was generously donated by Prof. Miles Houslay (University of Glasgow, UK). pcDNA3/HA-tagged wild type (WT) IκBα was generously donated by Prof. Warner Greene (Gladstone Institute of Virology and Immunology, University of California, San Francisco, CA). Sources of other materials have been described elsewhere (Palmer and Stiles, 1999).

Cell Culture. HUVECs were propagated in ECM-2 medium supplemented with 2% (w/v) fetal bovine serum, hydrocortisone, ascorbate, and recombinant growth factors as recommended by the supplier (Cambrex Bio Science Nottingham Ltd.). Human embryonic kidney 293 and C6 glioma cells were propagated in Dulbecco's modified Eagle's medium (DMEM) supplemented with 10% (v/v) fetal bovine serum, 1 mM L-glutamine, 100 units/ml penicillin and 100 μg/ml streptomycin. The generation and characterization of the C6 cell lines used in this study have been described elsewhere (Palmer and Stiles, 1999). All cells were grown at 37°C in a humidified atmosphere containing 5% (v/v) CO_2.

Generation of a Myc Epitope-Tagged Human A_{2A}AR. Myc epitope (EQKLISEEDL) and His_6 sequences were added to the carboxyl terminus of the human A_{2A}AR by PCR using pCMV5/human A_{2A}AR cDNA as the template. The primers were 5′-TAGCAGAGCTCGTTTAGT-3′, which anneals within pCMV5 upstream of the A_{2A}AR initiating Met, and 5′-TGAT**TCTAGA**GGACACTCCTGCTCCATCCTG-3′, which was designed to remove the A_{2A}AR stop codon and add a *Xba*I site (in bold). This was to allow in-frame fusion of the A_{2A}AR upstream of the myc epitope and His_6 sequences in pcDNA3/*myc*HisA (Invitrogen) after ligation of *Hind*III/*Xba*I-digested vector and similarly digested PCR product. The integrity of the generated open reading frame was verified by DNA sequencing.

Generation of Recombinant Serotype 5 AV Encoding myc-humA_{2A}AR. The myc-humA_{2A}AR open reading frame was excised from pcDNA3/mycHisA by *Hind*III/*Pme*I digestion and subcloned into *Hind*III/*EcoR*V-digested shuttle vector pAdTrackCMV: the subcloning procedure destroyed the *EcoR*V and *Pme*I sites. The resulting pAdTrackCMV/myc-humA_{2A}AR construct was then linearized at the remaining *Pme*I site within the vector to expose the inverted terminal repeats, and cotransformed with pAdEasy1 into *E. coli* strain BJ5183 by electroporation in 2.0 mm cuvettes at 2500V, 200Ω, and 25 μF. Successful pAdEasy1/myc-humA_{2A}AR recombinants were identified by *Pme*I digestion and PCR using myc-humA_{2A}AR-specific primers, and expanded in *E. coli* XL1 Blue. Plasmid DNA prepared from chosen clones was then digested with *Pac*I and transfected using LipofectAMINE into low-passage human embryonic kidney 293 cells to initiate viral production. Large-scale amplification and titration of AV/GFP and AV/myc-humA_{2A}AR viral stocks were performed as described by He et al. (1998).

For infection, HUVECs were washed in regular growth medium and then incubated overnight with the same medium supplemented with recombinant AV at the m.o.i. indicated under *Results* and figure legends. The next day, the virus-containing medium was aspirated and replaced with normal medium. Cells were used for analysis 24 h later.

Luciferase Assays of Reporter Gene Transcription in C6 Glioma Cells. C6 cells at 70 to 80% confluence in six-well dishes were transfected with 1 μg/well each of 3-κB enhancer conA-luciferase and pSVβ-galactosidase plasmids using 7 μl of GeneJuice according to the manufacturer's instruction. Forty-eight hours later, cells were treated as described in the figure legends. Reactions were terminated by placing on ice and washing twice with ice-cold PBS before harvesting by scraping into 50 μl of lysis buffer]50 mM potassium phosphate, pH 7.8, 0.2% (v/v) Triton X-100, and 0.5 mM DTT] that was clarified by centrifugation at 48,000*g* for 15 min. Fifteen microliters of the supernatant was used for determination of β-galactosidase activity according to manufacturer's instructions; 25 μl was added to luciferase assay buffer [50 mM Tris phosphate, pH 7.8, 16 mM magnesium chloride, 2 mM DTT, 1.8% (v/v) Triton X-100, and 30% (v/v) glycerol] for determination of luciferase activity in a 96-well luminometer plate. Samples were assayed in triplicate, and luciferase activity was normalized to β-galactosidase activity.

Transient Transfection of HUVECs. Endotoxin-free cDNA expression constructs were prepared using the Wizard Purefection plasmid DNA purification system (Promega). These were introduced into HUVECs using the Amaxa nucleofection kit according to the manufacturer's instructions. In brief, 1×10^6 HUVECs per sample were resuspended in 100 μl of nucleofection buffer containing 1 μg of pMaxGFP (to assess transfection efficiency) and 4 μg of either pcDNA3 (vector control) or pcDNA3/HA-tagged WT IκBα. Plasmid DNA was introduced into the nucleus of the cells using an Amaxa Nucleofector set at program U-O1. Cells were then seeded into 96-well plates, and E-selectin induction was assessed 48 h later by ELISA.

^{125}I-ZM241385 Synthesis and Saturation Binding. ^{125}I-ZM241385 was synthesized, purified by HPLC, and used in radioligand binding studies on freshly isolated HUVEC membranes as described by Palmer et al. (1995).

Monocyte Adhesion Assay. 1×10^4 HUVECs/well were seeded into a 24-well plate and grown overnight. The cells were then infected for 24 h at a m.o.i. of 25 pfu/cell with recombinant AVs. After treatment as indicated in the figure legends, the medium was aspirated, and HUVEC monolayers were overlaid with 1×10^5 U937 promonocytic cells/well. The cells were allowed to adhere for 1 h at 37°C before removal of the medium and washing of monolayers three times with 1 ml/well serum-free Dulbecco's modified Eagle's medium to remove any nonadherent U937 cells. The cells were then fixed in 0.5 ml/well 4% (w/v) paraformaldehyde in 5% (w/v) sucrose/PBS, pH 7.2, and analyzed using a combination of fluorescence and bright-field microscopy to determine the number of U937 cells adhering to GFP-expressing HUVECs. At least 300 GFP-expressing cells were counted in three to five separate fields to calculate the average number of adherent cells per 100 GFP-expressing HUVECs for any given treatment.

ELISA for Cell Surface E-Selectin Expression. 1×10^5 HUVECs/well were seeded in a 96-well plate and grown to 70% confluence. The cells were then infected for 24 h at a m.o.i. of 25 pfu/cell with recombinant AVs. The following day, cells were treated with TNFα for the times indicated in the figure legends. The incubation was stopped by transferring the plate to ice, and cells were washed gently three times with 0.2 ml/well ice-cold PBS. Cells were then fixed by overnight incubation at 4°C with 0.1 ml/well 4% (w/v) paraformaldehyde in 5% (w/v) sucrose/PBS, pH 7.2. The next day, each well was washed gently three times with PBS and then incubated for 1 h at room temperature in PBS containing 0.1% (w/v) BSA to block nonspecific antibody binding sites. After three more washes with PBS, 0.1 ml of anti-E-selectin antibody diluted 1:1000 in PBS/0.1% (w/v) BSA was added to each well. A parallel set of isotype control incubations using anti-hemagglutinin antibody 12CA5 at 1:1000 dilution was included to assess nonspecific antibody binding. After a 2-h incubation at room temperature, antibody solution was removed and the cells were washed three times with PBS before the addition of 0.1 ml/well horseradish peroxidase-conjugated anti-mouse IgG diluted 1:1000 in PBS/0.1% (w/v) BSA and incubation for 1 h at room temperature. Wells were then washed five times with PBS before the addition of 0.1 ml/well 3,3′,5,5′-tetramethylbenzidine. The reaction was allowed to develop at room temperature before A_{600} determination using a plate reader.

Griess Assay of Nitrite Accumulation. Confluent C6 cells in six-well plates were incubated in normal medium with the stimuli indicated in the figure legends. Synthesis of nitric oxide was determined by assay of culture supernatants for nitrite, a reaction product of nitric oxide and molecular oxygen. In brief, 0.2 ml of culture supernatant was allowed to react with 0.2 ml of Griess reagent (Hevel and Marletta, 1994) and incubated at room temperature for 15 min. After transfer to a 96-well plate, sample absorbance at 570 nm was determined using a plate reader. Fresh culture media served as the blank in all experiments, and nitrite concentrations from experimental samples were calculated from a standard curve derived from the parallel reaction of known amounts of sodium nitrite.

Immunoblotting. Confluent HUVECs or C6 cells in six-well plates were treated as described in the figure legends before washing in ice-cold PBS and solubilization by scraping into 0.2 ml/well electrophoresis sample buffer (50 mM Tris-HCl, pH 6.8, 10% (v/v) glycerol, 2% (w/v) SDS) at room temperature. After brief probe sonication, insoluble material was pelleted by microcentrifugation, and the supernatant was assayed for protein content using a bicinchoninic acid assay. Samples equalized for protein content (typically 50–70 μg/sample) were fractionated by SDS-PAGE on 10 or 12% (w/v) resolving gels. After transfer to nitrocellulose, membranes were blocked for 1 h at room temperature in blocking solution [5% (w/v) skimmed milk in PBS containing 0.1% (v/v) Tween 20]. Membranes were then incubated overnight at 4°C with primary antibody diluted in fresh blocking buffer. Primary antibodies were each used at used at a final concentration of 1 μg/ml. After three washes in blocking solution, membranes were incubated for 1 h at room temperature with appropriate horseradish peroxidase-conjugated secondary antibody at a 1 in 1000 dilution. After further washes with blocking buffer and PBS, immunoreactive proteins were visualized by enhanced chemiluminescence. For phosphospecific antibodies, a similar protocol was used except that the primary antibodies were diluted in Tris-buffered saline containing 1% (w/v) BSA and 0.1% (v/v) Tween 20, and all washes were with Tris-buffered saline/0.1% (v/v) Tween 20. Quantitation was by densitometric scanning of exposed films using Totallab imaging software (Phoretix; Nonlinear Dynamics, Newcastle upon Tyne, UK).

Pull-Down Assay of c-Jun N-Terminal Kinase Activation. Confluent C6 cells in six-well dishes were treated as indicated in the figure legends. Incubations were terminated by placing the cells on ice and washing in ice-cold PBS. All subsequent procedures were performed at 4°C unless indicated otherwise. Cells were solubilized in 0.3 ml/well c-Jun N-terminal kinase (JNK) lysis buffer (25 mM HEPES, pH 7.7, 20 mM β-glycerophosphate, 0.3 M sodium chloride, 1.5 mM magnesium chloride, 10 mM sodium fluoride, 0.1 mM sodium vanadate, 0.1 mM PMSF, and 10 μg/ml each of soybean trypsin inhibitor and benzamidine). After isolation of soluble fractions by microcentrifugation, samples equalized for protein content and volume were incubated overnight with rotation with 10 μg of recombinant GST-c-jun(1–79) immobilized to glutathione-Sepharose beads after induction and purification from transformed *E. coli* BL21 cultures. Complexes were isolated by brief microcentrifugation, washed three times with wash buffer [20 mM HEPES, 50 mM sodium chloride, 2.5 mM magnesium chloride, 0.1 mM EDTA and 0.05% (v/v) Triton X-100], and then resuspended in 30 μl of kinase assay buffer (25 mM HEPES, pH 7.5, 10 mM magnesium chloride, 20 mM β-glycerophosphate, and 75 mM sodium vanadate) supplemented with 100 μM ATP and 2 mM DTT. Immobilized JNK was activated by incubation at 30°C for 30 min. Reactions were stopped by the addition of 10 μl of 4× electrophoresis sample buffer containing 12% SDS and heating to 95°C for 5 min. Samples were fractionated by SDS-PAGE on 12% (w/v) polyacrylamide resolving gels and transferred to nitrocellulose for immunoblotting with anti-Ser^{63}-phosphorylated c-jun antibody for visualization of GST-c-Jun(1–79) phosphorylation. Protein-equalized samples from each treatment were also processed in parallel for immunoblotting with anti-JNK1,2 antibody.

Electrophoretic Mobility Shift Assay. After treatment as described in the figure legends, confluent 10-cm dishes of HUVEC or C6 cells were washed three times with ice-cold PBS before scraping. Cells were pelleted by centrifugation at 400*g* and lysed by the addition of 0.4 ml/tube buffer A [10 mM HEPES, pH 7.9, 10 mM potassium chloride, 0.1 mM EDTA, 0.1 mM EGTA, 1 mM DTT, 0.625% (v/v) Nonidet P-40, 0.5 mM PMSF, and 10 μg/ml each of soybean trypsin inhibitor and benzamidine]. The samples were then centrifuged at 48,000*g* for 30 s at 4°C, and the supernatant was removed. The pellet was resuspended in 50 μl of buffer B (20 mM HEPES, pH 7.9, 0.45 M sodium chloride, 1 mM EDTA, 1 mM EGTA, 1 mM DTT, 0.5 mM PMSF, and 10 μg/ml each of soybean trypsin inhibitor and benzamidine). Samples were agitated for 15 min at 4°C, centrifuged at 48,000*g* for 5 min, and the protein content of the supernatant was determined using a Bradford assay. Five-microliter samples from each nuclear extract were then added to a ^{32}P-labeled double-stranded DNA probe (10,000 cpm/sample) containing the consensus κB binding sequence GGGGACTTTCCC to give a final reaction volume of 25 μl containing 10 mM sodium HEPES, pH 7.9, 0.1 mM magnesium chloride, 0.1 mM EDTA, 0.5 mM DTT, 10% (v/v) glycerol, 50 mM sodium chloride, and 0.625 μg/ml poly(dIdC). After a 30-min incubation at room temperature, samples were analyzed by fractionation on a nondenaturing 6% (w/v) polyacrylamide gel containing 0.5× Tris-borate/EDTA buffer (45 mM Tris-borate, 1 mM EDTA) followed by autoradiography. For supershift analysis, 1 μl/sample of

sheep polyclonal anti-p65, anti-p50 antibodies, or nonimmune serum controls were added after the initial binding of the probe, and samples were incubated for a further 30 min at room temperature before electrophoresis.

Laser-Scanning Confocal Microscopy. 1×10^5 HUVECs were plated onto glass coverslips in six-well plates and cultured overnight. The next day, cells were treated as outlined in the figure legends, permeabilized by the addition of 0.4% (v/v) Triton X-100 in PBS for 3 min, then washed with PBS supplemented with 0.1% (v/v) goat serum and 0.2% (w/v) gelatin (PBSGG). Coverslips were then incubated with a 1:200 dilution of RelA/p65 antibody. After washing with three changes each of PBSGG and PBS, coverslips were incubated with at room temperature for 1 h in a 1:200 dilution of Alexa594-conjugated goat anti-rabbit IgG. After sequential washing with PBSGG and PBS as described above, coverslips were mounted onto glass slides using 40% (v/v) glycerol in PBS for dual-label confocal microscopy using a Zeiss AxioVERT 100 confocal microscope. Images were collected using dual excitation (488 and 543 nm) and emission (515–540 nm for GFP, and 590–610 nm for Alexa594) filter sets. Single labeled controls ensured that there was no interchannel bleed-through under these conditions. All collected images were analyzed using Metamorph software (Universal Imaging Corporation, Downingtown, PA).

Statistical Analysis. Data are presented in the text as means ± S.E. for the number of experiments indicated, whereas representative experiments are presented in the figures. Statistical significance was assessed using Student's t test or analysis of variance with a α probability of 0.05.

Results

Effect of A_{2A}AR Expression on iNOS Induction in C6 Glioma Cells. Glial cell inflammation plays an important role in the pathophysiology of Parkinson and Alzheimer diseases (Hirsch et al., 2003; Monsonego and Weiner, 2003). To determine the ability of the A_{2A}AR to regulate inflammatory responses in this cell type, rat C6 glioma cells stably expressing the canine A_{2A}AR to a range between 2 and 3 pmol/mg, as determined by saturation binding with the A_{2A}AR-selective antagonist radioligand ^{125}I-ZM241385, were used (Palmer and Stiles, 1999). The accumulation of nitrite and the associated induction of iNOS were used as inflammatory markers in this system, because iNOS-derived nitric oxide release contributes to the ability of activated glial cells to promote neuronal cell death (Brown and Bal-Price, 2003). Although no significant nitrite accumulation was observed when they were added individually, maximally effective concentrations of LPS, TNFα, or a combination of the two with IFNγ produced a marked induction of nitrite accumulation in control C6 cells that was abolished in A_{2A}AR-expressing C6 cells (nitrite accumulation in response to LPS/TNFα/IFNγ treatment for 24 h was reduced by 95 ± 9% in C6/A_{2A}AR cells versus control C6 cells, $n = 10$, $p < 0.05$; Fig. 1A). This was associated with an abolition of iNOS induction in response to LPS/TNFα/IFNγ even in the absence of the AR agonist NECA (Fig. 1B). The constitutive inhibition of iNOS induction observed is unlikely to be caused by the accumulation of extracellular adenosine acting on the recombinant receptor for two reasons. First, all cellular incubations presented in this study were performed in the presence of 3 units/ml adenosine deaminase to convert any released adenosine to inosine, which is inactived at the A_{2A}AR (Jin et al., 1997). Second, inhibition of iNOS induction could not be reversed significantly by inclusion of the A_{2A}AR-selective antagonist ZM241385 at a concentration that blocks specific binding to the A_{2A}AR [LPS/TNFα/IFNγ treatment produced a 12 ± 12% increase in nitrite accumulation in vehicle pretreated C6/A_{2A}AR cells versus 5 ± 15% in 1 μM ZM241385-pretreated cells, $n = 3$, $p > 0.05$ (not significant); Fig. 1C]. Therefore, it is possible that constitutive agonist-independent signaling from the A_{2A}AR is sufficient to block iNOS induction in C6 cells.

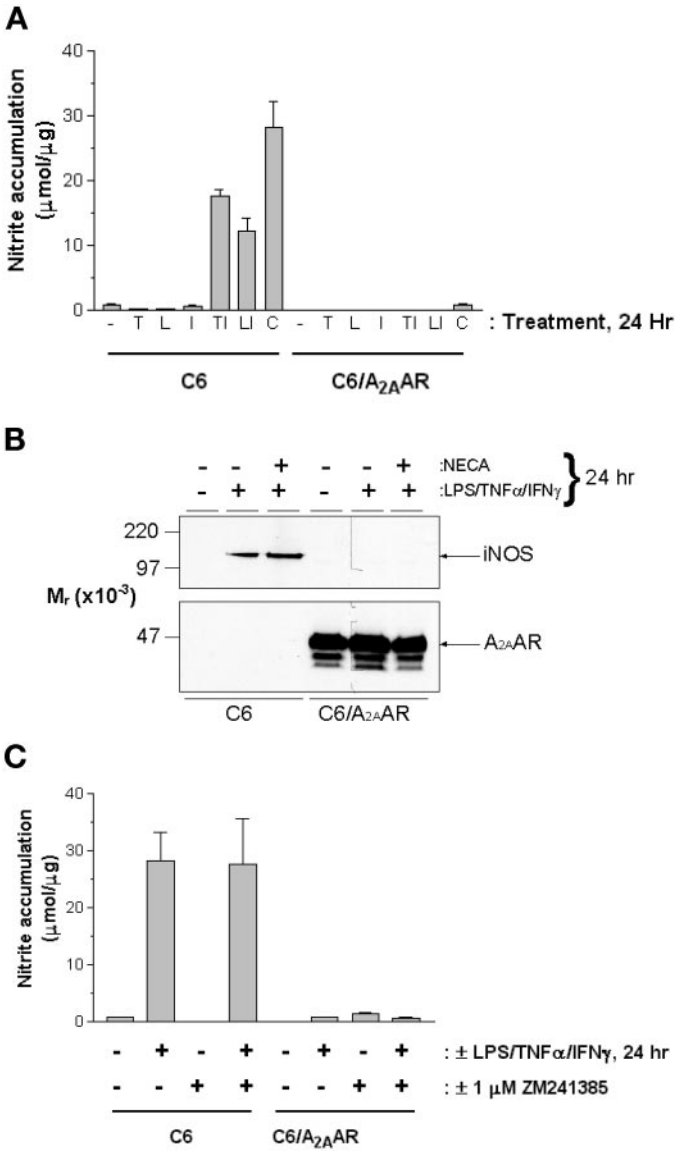

Fig. 1. Effect of A_{2A}AR expression on nitrite accumulation and iNOS induction in C6 glioma cells. A, control and A_{2A}AR-expressing C6 cells were treated for 24 h with 1 μg/ml LPS (L), 10 ng/ml TNFα (T), or 10 units/ml IFNγ (I) individually or in combination (LPS/TNFα/IFNγ) (C) before analysis of nitrite accumulation as described under *Materials and Methods*. This is one of multiple similar experiments. B, control and A_{2A}AR-expressing C6 cells were treated for 24 h with or LPS/TNFα/IFNγ in the absence of presence of 5 μM NECA. Detergent-soluble extracts from treated cells were then normalized for protein content before fractionation by SDS-PAGE and assessment of iNOS and A_{2A}AR expression by immunoblotting. This is one of multiple similar experiments. C, control and A_{2A}AR-expressing C6 cells were treated for 24 h with or without LPS/TNFα/IFNγ in the absence of presence of 1 μM ZM241385 as indicated. Samples were then analyzed for nitrite accumulation as described under *Materials and Methods*. This is one of multiple similar experiments.

The A_{2A}AR Acts Intracellularly to Inhibit iNOS Induction. In theory, it was possible that A_{2A}AR expression was leading to constitutive induction and secretion of anti-inflammatory cytokines or other signaling molecules that were acting extracellularly to inhibit iNOS induction. However, medium taken from A_{2A}AR-expressing C6 cells failed to inhibit LPS/TNFα/IFNγ induction of iNOS expression in control C6 cells (Fig. 2). In fact, medium from A_{2A}AR-expressing C6 cells actually potentiated iNOS induction by 62 ± 18% ($p < 0.05$, $n = 4$) compared with medium from control C6 cells (Fig. 2). Therefore, the A_{2A}AR must be acting intracellularly to block the signaling pathways leading to iNOS induction.

Effect of A_{2A}AR Expression on the Activation of the NF-κB, JNK, and p38 Pathways. Three key inflammatory signaling pathways activated in response to LPS and TNFα include the NF-κB pathway and the JNK and p38 stress-activated protein kinase signaling pathways (Manning and Davis, 2003; Kumar et al., 2003; Karin et al., 2004). Immunoblotting of extracts from TNFα-treated control and A_{2A}AR-expressing C6 cells with an antibody versus active phosphorylated p38 demonstrated that in both cell types, TNFα produced a transient activation of this kinase that peaked by 5 min and returned to basal by 30 min (Fig. 3A). Expression of the A_{2A}AR produced a 25 ± 6% ($p < 0.05$, $n = 3$) decrease in the maximal extent to which p38 was activated after normalization to total p38 expression. In vitro kinase assays of JNK activation demonstrated that A_{2A}AR expression had no significant effect on either the maximal extent of TNFα stimulation [maximal activation reduced by 9 ± 6% at 15 min, $p > 0.05$ (not significant), $n = 3$; Fig. 3B] or total JNK expression levels (Fig. 3B). Consistent with a minimal effect on JNK activation, TNFα stimulation of AP-1 activity, as determined after transient transfection of an AP1-luciferase reporter construct, was also not significantly different between control and A_{2A}AR-expressing C6 cells (data not shown).

Activation of the NF-κB pathway was assessed by two criteria. First, EMSAs were used to determine the ability of NF-κB to bind to target DNA. Stimulation with LPS and TNFα, but not IFNγ, for 60 min stimulated DNA binding in control C6 cells, but this was reduced by 85 ± 16% (TNFα) and 90 ± 11% (LPS) in A_{2A}AR-expressing cells (both $p < 0.05$ versus control C6 cells, $n = 3$; Fig. 4A). Supershift analysis revealed that both bands constituted p50-p65 heterodimers (data not shown). Second, to determine the functional consequences of reduced DNA binding, control and A_{2A}AR-expressing C6 cells were transfected with a 3-κB enhancer conA-luciferase reporter construct to assess NF-κB–mediated transcription. Although TNFα treatment for 6 h produced a 53.4 ± 3.6-fold increase in luciferase activity ($n = 5$) in control C6 cells, the fold-stimulation in A_{2A}AR-expressing C6 cells was only 4.3 ± 2.7 ($p < 0.05$ versus control C6 cells, $n = 5$; Fig. 4B). Therefore, A_{2A}AR expression selectively attenuated NF-κB-dependent gene transcription, and this was associated with a parallel reduction in NF-κB binding to target DNA.

Effect of NF-κB Inhibition on iNOS Induction. Several studies examining the promoter elements that control iNOS gene transcription have revealed the presence of multiple κB binding sites and demonstrated their importance for proper induction in response to inflammatory stimuli (Xie et

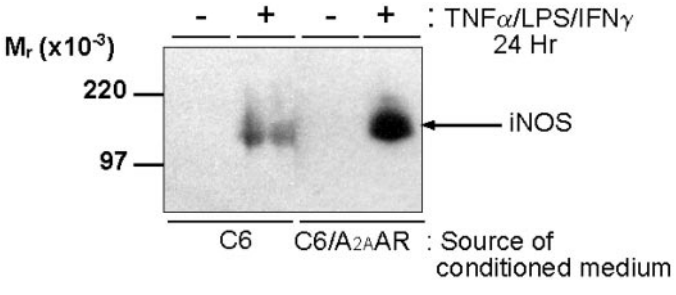

Fig. 2. Effect of conditioned medium from A_{2A}AR-expressing C6 glioma cells on iNOS induction in control C6 glioma cells. Fresh medium was added to confluent dishes of control and A_{2A}AR-expressing C6 cells. After 24 h, the medium from each dish was removed, supplemented with LPS/TNFα/IFNγ or not, and added to confluent monolayers of control C6 cells for a further 24 h as described in Fig. 1. Protein-normalized soluble extracts were then prepared and fractionated by SDS-PAGE for immunoblot analysis of iNOS induction. This is one of multiple experiments.

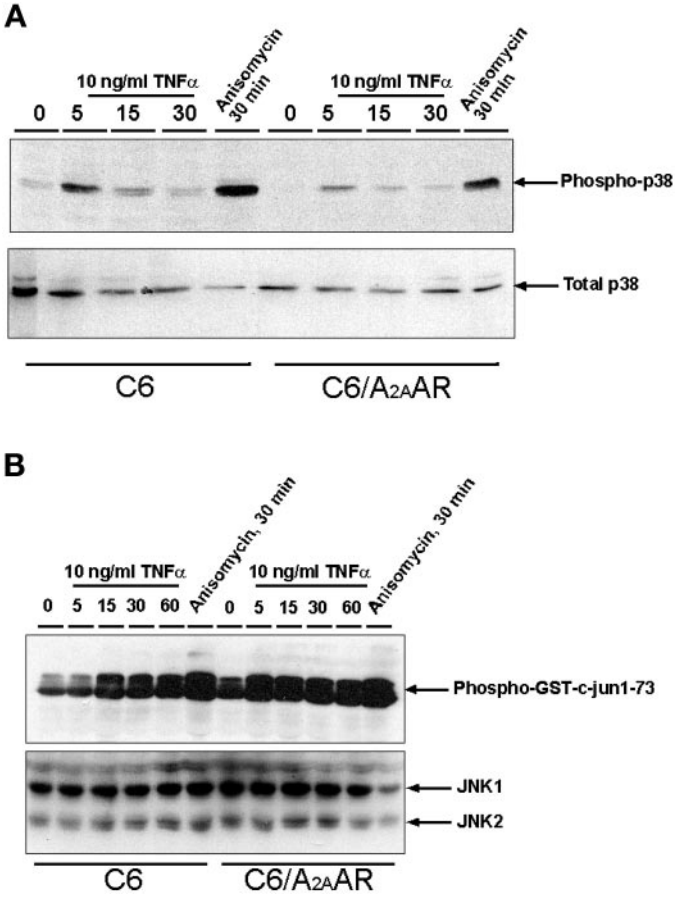

Fig. 3. Effect of A_{2A}AR expression on TNFα stimulation of p38 phosphorylation and JNK activation in C6 glioma cells. A, control and A_{2A}AR-expressing C6 glioma cells were treated with or without 10 ng/ml TNFα or 5 μg/ml anisomycin for the indicated times before preparation of soluble cell extracts. After normalization for protein content, duplicate samples were fractionated by SDS-PAGE and transferred to nitrocellulose for parallel immunoblotting with Thr^{180}/Tyr^{182}phospho-specific and total anti-p38 antibodies as described under *Materials and Methods*. B, control and A_{2A}AR-expressing C6 glioma cells were treated with or without 10 ng/ml TNFα or 5 μg/ml anisomycin for the indicated times before preparation of soluble cell extracts. After normalization for protein content, samples were assayed for JNK activation by incubation with glutathione-Sepharose-bound GST-c-Jun(1–79) and assay of the pulled down kinase. Phosphorylation of GST-c-Jun(1–79) was assessed by SDS-PAGE and immunoblotting with a Ser^{63}phospho-specific c-Jun antibody and parallel immunoblotting of treated cell extracts with anti-JNK1,2 antibody as described under *Materials and Methods*.

al., 1994; Taylor and Geller, 2000). Given that the effects of $A_{2A}AR$ expression on p38 and JNK activation were minimal compared with the effect on NF-κB function, it was likely that the inhibition of iNOS induction observed (Fig. 1) could be accounted for by the effects of $A_{2A}AR$ on the NF-κB pathway. To test this hypothesis, C6 cells were preincubated with the NF-κB inhibitor pyrrolidine dithiocarbamate (PDTC) before 24-h treatment with or without LPS/TNFα/IFNγ and assessment of nitrite accumulation in the medium (Dai et al., 2003). Preincubation with PDTC attenuated nitrite accumulation by 55 ± 7% ($p < 0.05$, $n = 3$) compared with C6 cells pretreated with an antioxidant control compound [*N*-acetylcysteine (NAcCys)] (Fig. 5A). An alternative strategy was also employed to assess the effects of NF-κB inhibition on nitrite accumulation. In particular, control C6 cells were transfected with a wild-type IκBα expression construct before stimulation with LPS/TNFα/IFNγ (Fig. 5B). Expression of recombinant IκBα inhibits NF-κB function by sequestering liberated NF-κB dimers, thereby preventing their nuclear translocation and subsequent binding to target DNA (Sun et al., 1996). Compared with vector-transfected C6 cells, nitrite accumulation was reduced by 68 ± 15% in IκBα-transfected cells ($n = 3$, $p < 0.05$, Fig. 5B). Together, these data suggest that inhibition of NF-κB caused by $A_{2A}AR$ expression could at least partly explain the receptor's ability to attenuate iNOS induction.

Effect of $A_{2A}AR$ Expression on IκBα Regulation in C6 Cells. TNFα and LPS each activate NF-κB by initiating the degradation of IκBα, which allows p50-p65 heterodimers to translocate to the nucleus and initiate transcription after a series of phosphorylation and acetylation reactions on p65 (Karin et al., 2004). IκBα phosphorylation on serines 32 and 36 by the IκB kinase (IKK) complex triggers its polyubiquitination by the $SCF^{\beta TrCP}$ complex and subsequent degradation by the 26S proteosome. In control C6 cells, TNFα was able to initiate a marked reduction in IκBα protein with kinetics similar to those observed by other investigators (Wang et al., 1999; Fig. 6A). However, in $A_{2A}AR$-expressing cells, the observed degradation of IκBα in response to TNFα was significantly reduced (at 30 min, IκBα reduction in control C6 cells

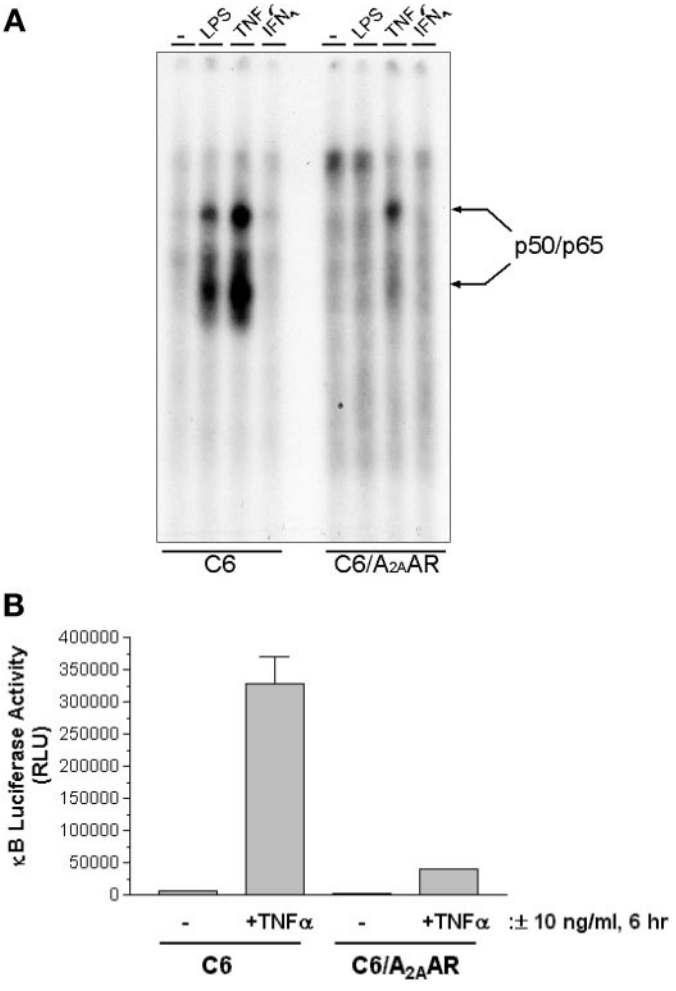

Fig. 4. Effect of $A_{2A}AR$ expression on NF-κB activation in C6 glioma cells. A, control and $A_{2A}AR$-expressing C6 glioma cells were treated with or without 10 ng/ml TNFα, 1 μg/ml LPS, or 10 units/ml IFNγ for 60 min before isolation of nuclei for electrophoretic mobility shift assay analysis with a κB-selective oligonucleotide probe as described under *Materials and Methods*. This is one of multiple experiments. B, control and $A_{2A}AR$-expressing C6 glioma cells were cotransfected with a κB-luciferase reporter construct and pSVβ-galactosidase. Forty-eight hours after transfection, cells were treated with or without TNFα as indicated, and extracts were prepared for assay of luciferase and β-galactosidase activities and normalization with respect to transfection efficiency and protein content as described under *Materials and Methods*. This is one of multiple experiments.

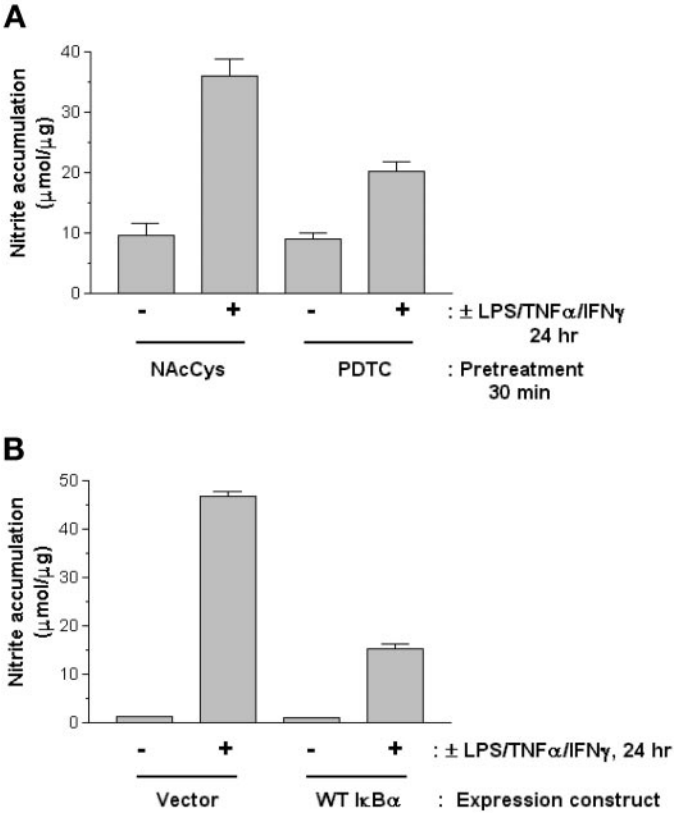

Fig. 5. Effect of NF-κB inhibition on nitrite accumulation in C6 glioma cells. A, control C6 glioma cells were pretreated with or without 100 μM PTDC or NAcCys for 30 min before the addition of vehicle or LPS/TNFα/IFNγ for a further 24 h as indicated. Medium from treated cells was then analyzed for nitrite accumulation as described under *Materials and Methods*. This is one of multiple experiments. B, control C6 glioma cells were transfected with either pcDNA3 vector or pcDNA3/HA-tagged WT IκBα as indicated. Twenty-four hours after transfection, cells were treated with LPS/TNFα/IFNγ for a further 24 h as indicated. Medium from treated cells was then analyzed for nitrite accumulation as described under *Materials and Methods*. This is one of multiple experiments.

was 84 ± 12% versus 20 ± 5% in A_{2A}AR-expressing C6 cells, $p < 0.05$, $n = 3$; Fig. 6A). Immunoblotting with an antibody that specifically recognized $Ser^{32}Ser^{36}$-phosphorylated IκBα revealed that this was associated with almost complete abolition of IκBα phosphorylation (phosphorylation after a 15-min exposure to TNFα reduced by some 83 ± 8% in A_{2A}AR-expressing C6 cells versus controls, $p < 0.05$, $n = 3$, Fig. 6A). A similar inhibition of IκBα degradation and phosphorylation was observed in response to LPS treatment, with $Ser^{32}Ser^{36}$ phosphorylation of IκBα after 15 min being reduced by 75 ± 11% in A_{2A}AR-expressing C6 cells versus controls, $p < 0.05$, $n = 3$, (Fig. 6B). Hence, the ability of the A_{2A}AR to inhibit NF-κB activation in response to TNFα and LPS is probably caused by inhibition of IκBα phosphorylation by the upstream IKK complex.

Effect of A_{2A}AR Activation on Monocyte Adhesion to TNFα-Stimulated HUVECs in Vitro. To determine whether the molecular mechanisms by which the A_{2A}AR inhibited inflammatory responses in C6 cells were conserved between different cell types, the effects of A_{2A}AR gene transfer were also assessed in HUVECs, a cell line whose responses to stimuli such as TNFα and LPS are well characterized. Several reports have suggested that ECs express low levels of endogenous A_{2A}ARs (Sexl et al., 1997; Feoktistov et al., 2002; Wyatt et al., 2002). To assess the ability of these receptors to inhibit inflammatory responses in HUVECs in vitro, cells were pretreated with a maximally effective concentration of the A_{2A}AR-selective agonist CGS21680 before treatment with increasing concentrations of TNFα and quantitation of U937 monocyte adhesion. Whereas maximally effective concentrations of TNFα increased U937 adhesion by 148 ± 25-fold ($n = 5$ experiments) with an EC_{50} of 0.37 ± 0.21 ng/ml, pretreatment with 5 μM CGS21680 increased the EC_{50} to 2.00 ± 0.88 ng/ml, thereby reducing monocyte adhesion at submaximal concentrations of TNFα (adhesion observed at 1 ng/ml TNFα reduced by 51 ± 14% $n = 3$, by 5 μM CGS21680 versus vehicle-treated HUVECs, $p < 0.05$; Fig. 7, A and B). Pharmacological analysis of this effect demonstrated that whereas the effect of CGS21680 was blocked completely by the A_{2A}AR-selective antagonist ZM241385, it could not be mimicked by the A_1AR-selective agonist CPA,

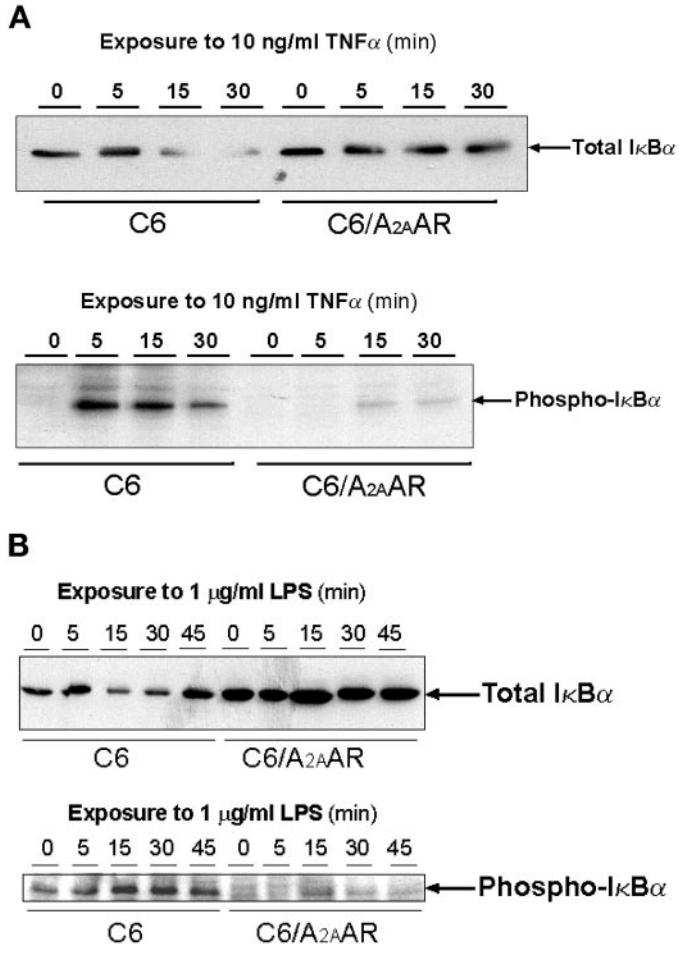

Fig. 6. Effect of A_{2A}AR expression on agonist-stimulated IκBα phosphorylation and degradation in C6 glioma cells. A, control and A_{2A}AR-expressing C6 glioma cells were treated with or without 10 ng/ml TNFα for the indicated times before preparation of detergent-soluble extracts. Samples equalized for protein content were fractionated by SDS-PAGE for immunoblotting with anti-IκBα (*upper*) or anti-$Ser^{32}Ser^{36}$phospho-IκBα (*lower*) antibodies as described under *Materials and Methods*. This is one of multiple experiments. B, control and A_{2A}AR-expressing C6 glioma cells were treated with or without 1 μg/ml LPS for the indicated times before preparation of detergent-soluble extracts. Samples equalized for protein content were fractionated by SDS-PAGE for immunoblotting with anti-IκBα (*upper*) or anti-$Ser^{32}Ser^{36}$phospho-IκBα (*lower*) antibodies as described above. This is one of multiple experiments.

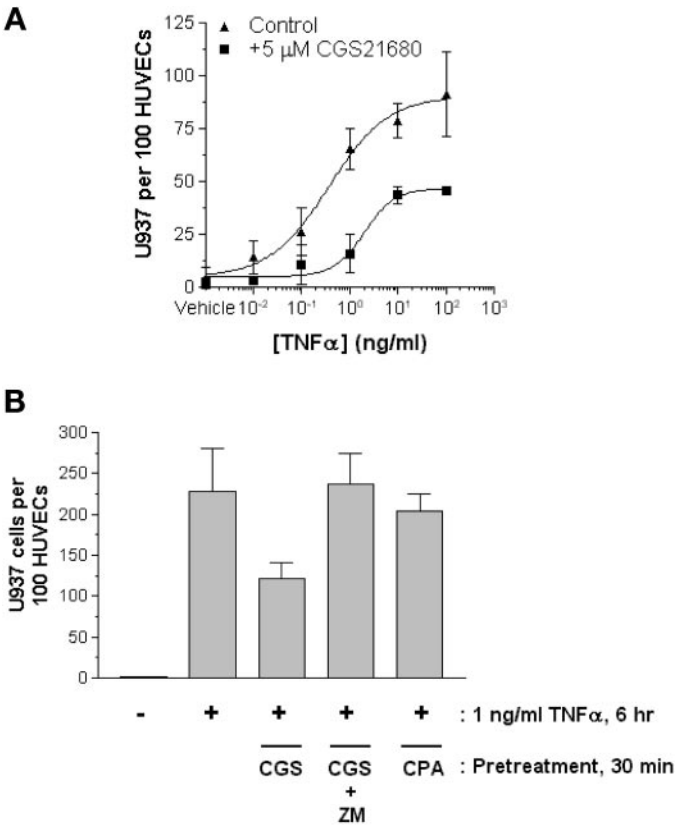

Fig. 7. Effect of endogenous A_{2A}AR activation on monocyte adhesion to TNFα stimulated HUVECs in vitro. A, confluent HUVEC monolayers were pretreated for 30 min with 5 μM CGS21680 before incubation with increasing concentrations of TNFα for 6 h as indicated. U937 promonocytic cells were then overlaid and the number of adherent cells quantitated as described under *Materials and Methods*. This is one of multiple experiments. B, confluent HUVEC monolayers were pretreated for 30 min with 5 μM CGS21680 (CGS), 5 μM CGS21680, and 1 μM ZM241385 (CGS+ZM) or 5 μM N^6-cyclopentyladenosine (CPA) as indicated before treatment with or without 10 ng/ml TNFα for 6 h and assessment of U937 adhesion as described under *Materials and Methods*. This is one of multiple experiments.

which is indicative of an A_{2A}AR-mediated phenomenon (Fig. 7B).

Effect of A_{2A}AR Gene Transfer on Monocyte Adhesion to TNFα-Stimulated HUVECs in Vitro. To assess whether it was possible to potentiate the anti-inflammatory effects of the A_{2A}AR, HUVECs were infected with recombinant AV encoding a myc epitope-tagged human A_{2A}AR with the aim of increasing receptor expression. The AV also expressed GFP from a separate open reading frame to facilitate identification of successfully infected cells by fluorescence microscopy. By this approach, it was possible to achieve recombinant protein expression in approximately 90% of infected HUVECs at optimal m.o.i. (Fig. 8A) with A_{2A}AR expression reaching 0.34 ± 0.06 pmol/mg of protein ($n = 3$ experiments) as determined by saturation binding analysis using ^{125}I-ZM241385 (Fig. 8B). It is interesting that despite unequivocal identification of functional A_{2A}ARs (Fig. 7), no specific binding of ^{125}I-ZM241385 was detectable in either uninfected or control AV/GFP-infected HUVECs. A similar inability to detect low level endogenous functional A_{2A}ARs by radioligand binding has also been reported for T-lymphocytes (Armstrong et al., 2001).

Experiments performed in C6 cells suggested that A_{2A}AR expression was sufficient to inhibit inflammatory responses even in the absence of agonist. To determine whether this was also a feature of endothelial cells, U937 adhesion assays were performed on TNFα-treated HUVECs infected with either AV/GFP or AV/myc-humA_{2A}AR (Fig. 9). Whereas TNFα strongly promoted monocyte adhesion in control GFP-expressing cells, expression of the A_{2A}AR inhibited this effect by 84 ± 8% ($n = 3$, $p < 0.05$ versus TNFα-treated HUVECs infected with control AV/GFP), and this was not improved substantially by the presence of the AR agonist NECA (89 ± 8% inhibition, $n = 3$, $p < 0.05$ versus TNFα- and NECA-treated HUVECs infected with control AV/GFP; Fig. 9).

Effect of A_{2A}AR Gene Transfer on E-Selectin Induction in HUVECs. Adherence of leukocytes to inflamed endothelium is mediated by specific adhesion molecules on both cell types. E-selectin is a key molecule on the EC surface responsible for initial recruitment of leukocytes out of the circulation before their arrest and diapedesis into underlying tissue (Ley, 2001). In agreement with several other studies, exposure of control AV-infected HUVECs to either TNFα for 6 h induced E-selectin expression at the cell surface (Oitzinger et al., 2001; Fig. 10A). A_{2A}AR gene transfer reduced the TNFα-mediated increase in cell surface E-selectin by 76 ± 5% ($n = 3$, $p < 0.05$ versus TNFα-treated AV/GFP-infected HUVECs; Fig. 10A). Moreover, this effect was not restricted to TNFα, because induction of E-selectin after a 4-h stimulation with LPS was similarly reduced (80 ± 12%, $n = 3$, $p < 0.05$ versus LPS-treated AV/GFP-infected HUVECs; Fig. 10B) as determined by immunoblotting. Thus, A_{2A}AR expression is sufficient to inhibit both E-selectin induction and monocyte adhesion.

Effect of NF-κB Inhibition on E-Selectin Induction and Monocyte Adhesion. Analysis of the human E-selectin

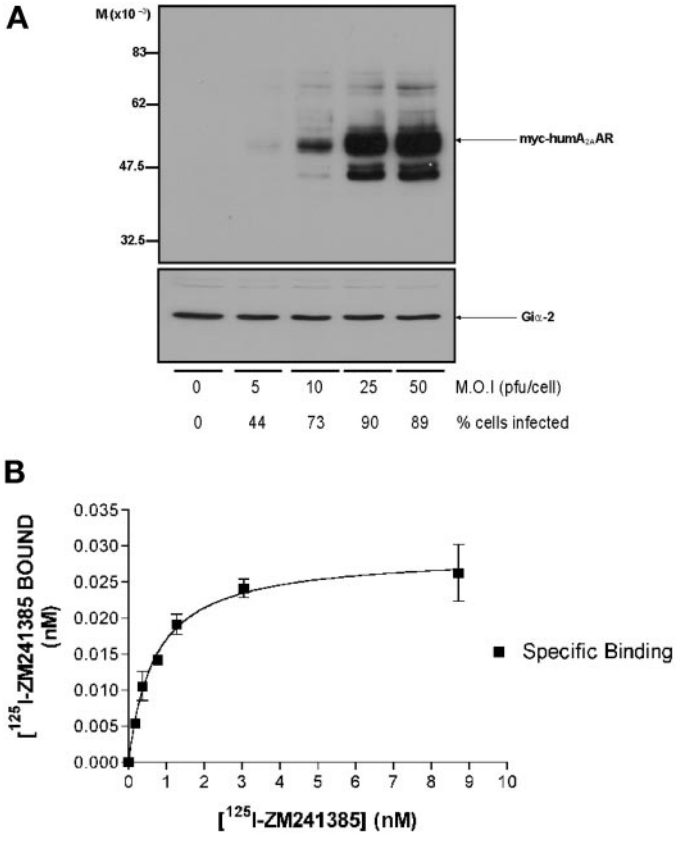

Fig. 8. Adenovirus-directed expression of the human A_{2A}AR in HUVECs. A, HUVECs were infected with AV/myc-human A_{2A}AR at the indicated m.o.i. as described under *Materials and Methods*. After the isolation of detergent-soluble extracts, samples were equalized for protein content and fractionated by SDS-PAGE for immunoblotting with anti-myc epitope antibody 9E10 to specifically identify recombinant receptor. Blots were then stripped and reprobed with an antibody versus $G_i\alpha$-2, to ensure equivalent protein loading in each lane. Determination of "% cells infected" was derived from counting the number of GFP-expressing cells by fluorescence microscopy and the total number of cells by light microscopy within five different fields. This is one of multiple experiments. B, membranes prepared from HUVECs infected with 25 pfu/cell AV/myc-human A_{2A}AR were subjected to saturation binding analysis using the A_{2A}AR-selective antagonist radioligand ^{125}I-ZM241385 as described under *Materials and Methods*. This is one of multiple experiments.

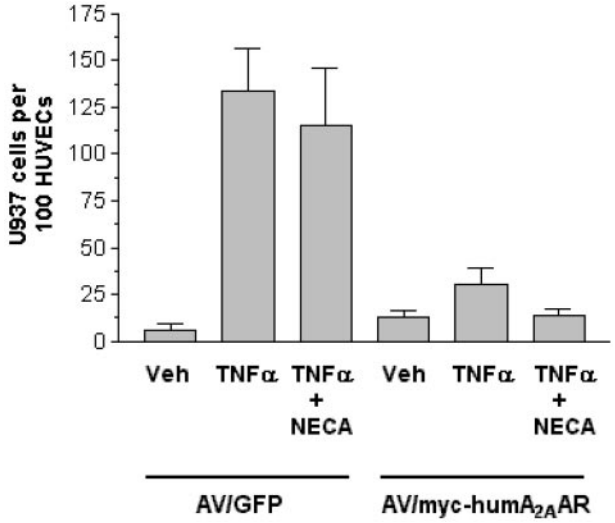

Fig. 9. Effect of A_{2A}AR gene transfer on monocyte adhesion to TNFα-pretreated HUVECs in vitro. HUVECs were infected with AV/myc-human A_{2A}AR at an m.o.i. of 25 pfu/cell as described under *Materials and Methods*. After pretreatment for 30 min with or without 5 μM NECA, cells were incubated with 10 ng/ml TNFα for 6 h as indicated. U937 cells were then overlaid and the number of adherent cells quantitated as described under *Materials and Methods*. This is one of multiple experiments.

promoter has identified four positive regulatory domains (termed PDI to -IV) responsible for conferring induction in response to inflammatory stimuli (Read et al., 1997). PDs I, III, and IV are κB-binding sites, whereas PDII is an AP-1 site at which an ATF2/c-jun heterodimer is constitutively bound. Thus, maximal induction arises from occupation of the κB-binding sites by NF-κB as well as p38- and JNK-mediated phosphorylation of ATF2 and c-jun, respectively (Read et al., 1997). The ability of TNFα to promote E-selectin induction in HUVECs was found to be dependent on κB binding rather than AP-1 activation, as HUVEC pretreatment with the NF-κB inhibitor PDTC inhibited induction by 87 ± 10% under conditions in which the p38 inhibitor SB203580 had no significant effect [7 ± 16% increase versus nonpretreated cells, $p > 0.05$ (not significant), $n = 3$; Fig. 11A). It is important that the effect of PDTC could not be explained by its antioxidant properties, because parallel treatment with the anti-oxidant NAcCys had minimal effects on E-selectin induction [6 ± 10% increase versus nonpretreated cells, $p > 0.05$ (not significant), $n = 3$, Fig. 11A]. Consistent with other investigators (Read et al., 1997), inhibition of the extracellular signal-regulated kinase signaling pathway using the mitogen-activated protein kinase kinase inhibitor U0126 also had no effect on induction [6 ± 7% increase versus nonpretreated cells, $p > 0.05$ (not significant), $n = 3$; Fig. 11A]. Again, to confirm a role for NF-κB, HUVECs were transfected with a WT IκBα expression construct before stimulation with TNFα and measurement of E-selectin induction. These experiments demonstrated that compared with vector-transfected cells, IκBα expression reduced TNFα-stimulated E-selectin induction by 72 ± 7% ($n = 3$, $p < 0.05$ versus vector-transfected controls; Fig. 11B). It is noteworthy that the observed reduction in E-selectin observed after inhibition of NF-κB was associated with a parallel inhibition of U937 adhesion to TNFα-stimulated HUVECs in vitro (PDTC produced a 88 ± 9% versus 25 ± 10% inhibition of adhesion in NAcCys-treated cells, $n = 4$, $p < 0.05$; Fig. 11C).

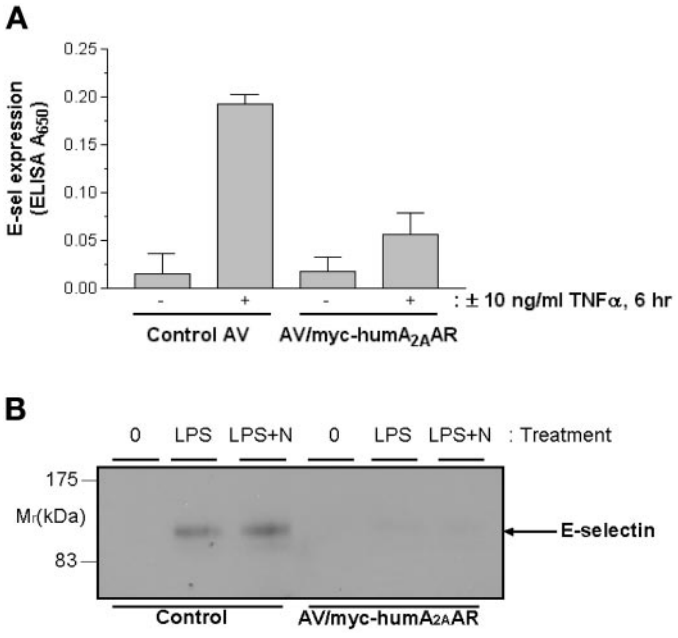

Fig. 10. Effect of A_{2A}AR gene transfer on TNFα- and LPS-mediated induction of E-selectin expression. A, HUVECs were infected with either AV/GFP (control AV) or AV/myc-human A_{2A}AR at an m.o.i. of 25 pfu/cell as described under *Materials and Methods*. After pretreatment with or without 10 ng/ml TNFα for 6 h, cell surface E-selectin expression was determined by ELISA as described under *Materials and Methods*. This is one of multiple experiments. B, HUVECs were infected with either AV/GFP (control AV) or AV/myc-human A_{2A}AR at an m.o.i. of 25 pfu/cell as described under *Materials and Methods*. After treatment in the absence (0) or presence of 1 μg/ml LPS either alone (LPS) or with 5 μM NECA (LPS+N) for 4 h, cell surface E-selectin expression was determined by immunoblotting as described under *Materials and Methods*. This is one of multiple experiments.

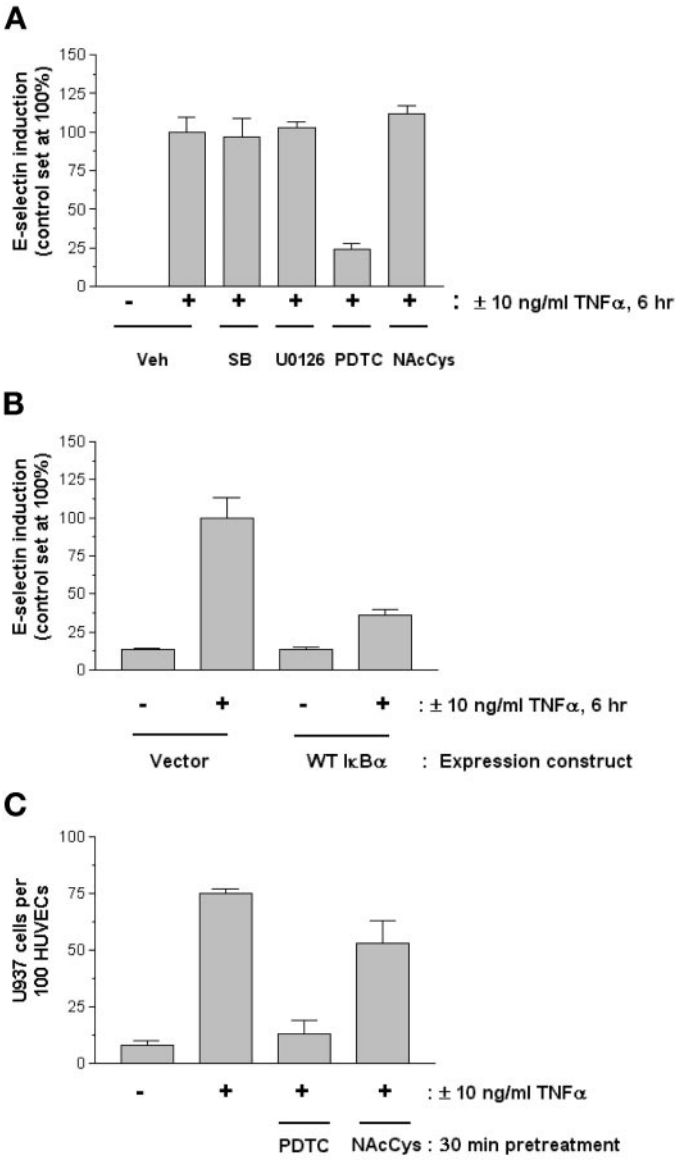

Fig. 11. Effect of NF-κB inhibition on TNFα-mediated induction of E-selectin and monocyte adhesion in HUVECs. A, confluent HUVECs in a 96-well plate were incubated with or without 10 ng/ml TNFα after a 30-min preincubation in the absence or presence of 10 μM SB203580, 10 μM U0126, 100 μM PDTC, or 100 μM NAcCys. Quantitation of E-selectin induction was by ELISA as described under *Materials and Methods*. This is one of multiple experiments. B, HUVECs were transfected with pMaxGFP and either pcDNA3 vector or pcDNA3/HA-tagged WT IκBα, seeded into a 96-well plate and cultured for 48 h as described under *Materials and Methods*. Cells were then treated with or without 10 ng/ml TNFα for 6 h before quantitation of E-selectin induction by ELISA. This is one of multiple experiments. C, confluent HUVEC monolayers were pretreated for 30 min with either 100 μM PDTC or NAcCys as indicated before stimulation with 10 ng/ml TNFα for 6 h. U937 cells were then overlaid and the number of adherent cells quantitated as described the *Materials and Methods*. This is one of multiple experiments.

Effect of A_{2A}AR Gene Transfer on NF-κB Regulation in HUVECs. The above experiments demonstrated that, similarly to C6 glioma cells, the anti-inflammatory effects of the A_{2A}AR in HUVECs could be largely mimicked by inhibition of NF-κB signaling. To determine whether A_{2A}AR gene transfer could also inhibit NF-κB binding to target DNA in HUVECs, EMSAs were performed on TNFα-treated cells after infection with either AV/GFP or AV/myc-humA_{2A}AR (Fig. 12A). These demonstrated that the ability of TNFα to promote p50-p65 heterodimer binding to target DNA was reduced by 86 ± 15% upon A_{2A}AR gene transfer ($n = 5$, $p < 0.05$ versus TNFα-treated AV/GFP-infected HUVECs; Fig. 12A).

Translocation of NF-κB to the nucleus is triggered by the phosphorylation-dependent degradation of the IκB proteins that maintain NF-κB in the cytoplasm (Karin et al., 2004). Expression of the A_{2A}AR in C6 cells severely attenuated IκBα phosphorylation on Ser^{32} and Ser^{36}, the two sites whose phosphorylation by the IKK complex is required for polyubiquitination and subsequent degradation by the proteosome (Fig. 6). However, despite unequivocal evidence of AV-directed A_{2A}AR expression in HUVECs, the ability of TNFα to trigger the degradation of IκBα was unaffected [degradation compared with vehicle-treated control at 15 min was 94 ± 6% (AV/GFP) versus 89 ± 10% (AV/myc-humA_{2A}AR), $n = 3$, $p > 0.05$ (not significant); Fig. 12B], suggesting that the mechanisms by which the A_{2A}AR inhibits NF-κB signaling differ between C6 glioma and HUVEC systems.

To determine whether the nuclear translocation of NF-κB was altered despite normal IκBα degradation, confocal laser-scanning microscopy was performed to analyze the subcellular distribution of p65 in AV-infected HUVECs after treatment with or without TNFα (Fig. 12C). Under unstimulated conditions, p65 resided in the cytoplasm in both sets of AV-infected cells. However, although stimulation with TNFα promoted the nuclear translocation of p65 in controls, p65 was excluded from the nucleus of A_{2A}AR-expressing HUVECs (Fig. 12C). Hence, A_{2A}AR gene transfer in HUVECs profoundly inhibits the ability of NF-κB p50-p65 heterodimers to bind target DNA and this is associated with a parallel reduction in p65 translocation to the nucleus in the absence of any effect on IκBα degradation

Discussion

The A_{2A}AR has been identified as a protective anti-inflammatory receptor protein not only from numerous pharmacological studies (reviewed in Linden, 2001) but also from characterization of inflammatory responses in mice in which both copies of the A_{2A}AR gene have been deleted (Ohta and Sitkovsky, 2001). Gene dosage studies have provided evidence to show that, at least in T-lymphocytes, there is no A_{2A}AR reserve (Armstrong et al., 2001). Therefore, pathophysiological conditions that alter A_{2A}AR expression, such as the onset of hypoxia (Kobayashi and Millhorn, 1999) and EC exposure to Th1 cytokines (Nguyen et al., 2003), are likely to alter cellular responsiveness to inflammatory stimuli. However, despite unequivocal evidence of its potent anti-inflammatory properties across different cell types, the molecular basis for the anti-inflammatory effects of A_{2A}AR have not been examined in detail. To begin addressing some of these issues, we have focused on characterizing the effects of increasing A_{2A}AR expression on glial and EC model systems, each of which is associated with multiple inflammatory diseases.

iNOS induction is a well characterized marker of glial cell inflammation (Brown and Bal-Price, 2003). Stable expression of the A_{2A}AR in C6 glioma cells was sufficient to abolish induction of iNOS expression and NF-κB activation. Moreover, this abolition did not require the presence of agonist and was not reversed by preincubation with the A_{2A}AR-selective antagonist ZM241385, suggesting that in this system, the receptor displays some agonist-independent basal activity. A similar phenomenon was also observed for monocyte adhesion, E-selectin induction, and NF-κB activation in HUVECs upon A_{2A}AR expression to a level of only 0.3 to 0.4 pmol/mg, suggesting that agonist-independent signaling may be an intrinsic property of the A_{2A}AR. Consistent with this hypothesis, constitutive A_{2A}AR activation of either cAMP production or the extracellular signal-regulated kinase pathway in the absence of agonist has been observed in other studies (Ledent et al., 1992; Klinger et al., 2002). However, both this study and others describing agonist-independent signaling from the A_{2A}AR have been cell systems in which the recombinant receptor is overexpressed. Therefore, the physiological significance in vivo of any basal activity of endogenous A_{2A}ARs expressed at low levels is unclear and will require the development of an A_{2A}AR-selective inverse agonist. Despite this caveat, when considered in the context of our observations, the increases in A_{2A}AR expression and function seen upon cytokine treatment or hypoxia in multiple cell types (Kobayashi and Millhorn, 1999; Khoa et al., 2001; Nguyen et al., 2003) probably constitute important negative feedback mechanisms that prevent the development of an excessive and inappropriate inflammatory response. The availability of A_{2A}AR-deficient mice can now allow quantitative assessment of the presence and importance of such a negative feedback loop in individual inflammatory cells.

A major finding from our experiments was that the pronounced inhibition of TNFα- and LPS-mediated inflammatory responses could be explained by a suppressive effect of A_{2A}AR expression specifically on the NF-κB pathway rather than the parallel p38 and JNK stress-activated kinase modules. However, whereas expression of the A_{2A}AR in glial cells blocked the IKK-mediated IκBα phosphorylation on Ser^{32} and Ser^{36} that triggers its degradation, IκBα degradation was unaffected upon A_{2A}AR expression in endothelial cells. Thus, the A_{2A}AR is able to inhibit the NF-κB pathway at multiple postreceptor loci common to TNFα and LPS/Toll-like receptor 4 (TLR4) signaling. In C6 cells, this locus must reside at a site at which TLR4 and TNF receptor signaling converge to activate NF-κB. The most likely candidates include components of the IKK complex (particularly IKKβ and IKKγ/NEMO) as well as any IKK kinases activated by both LPS and TNFα.

In terms of receptor pharmacology, we found that activation of endogenous A_{2A}ARs on HUVECs by the selective agonist CGS21680 was able to significantly inhibit monocyte adhesion, whereas the nonselective AR agonist NECA was not (Figs. 7 and 9). At the concentration used (5 μM), NECA activates all four AR subtypes (Fredholm et al., 2001). Several studies have demonstrated that both A_{2A}- and A_{2B}ARs are predominantly expressed in endothelial cells. Although both receptors share an ability to elevate cAMP levels via interaction with G_s, the A_{2B}AR can also couple to $G_{q/11}$ to

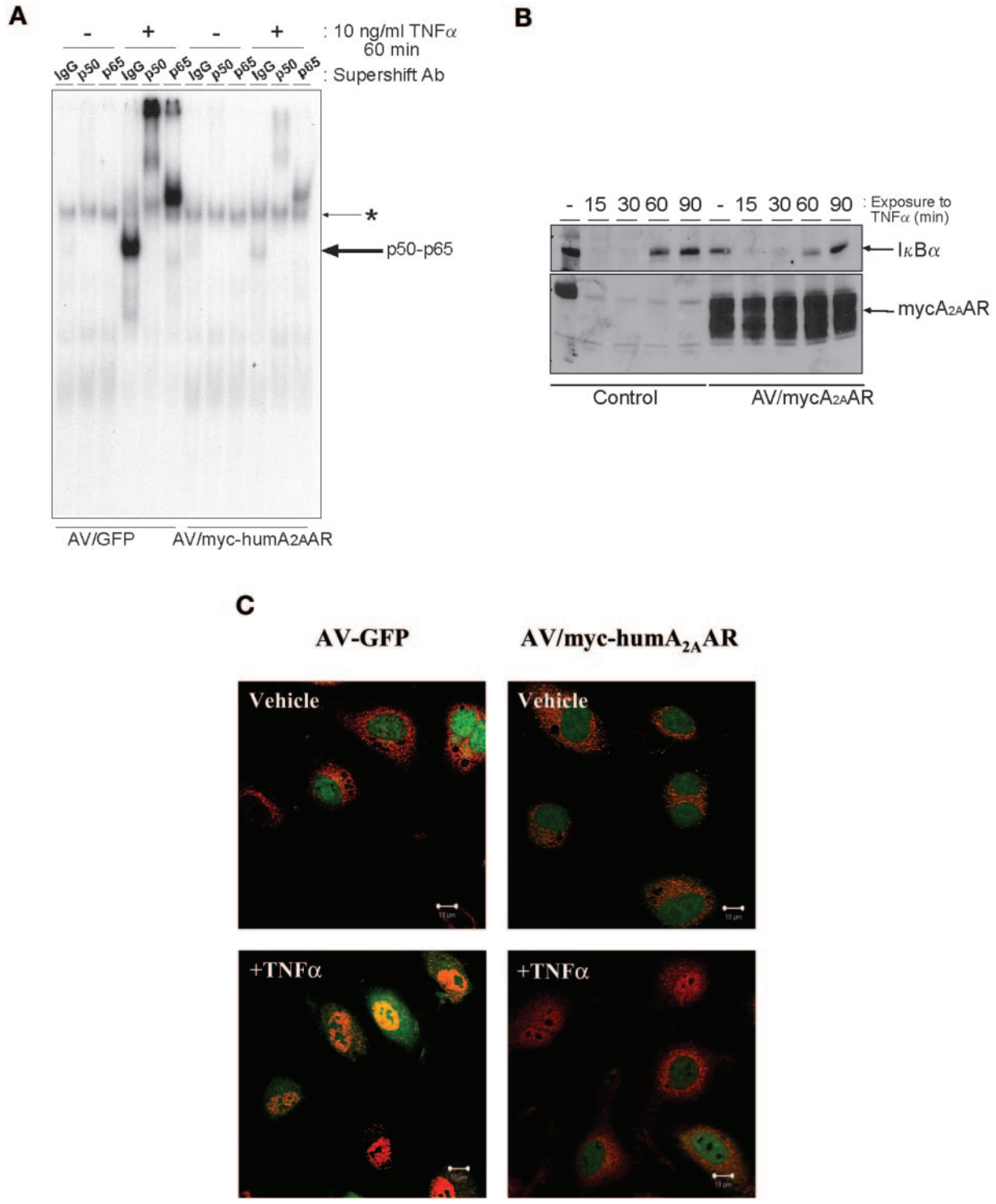

Fig. 12. Effect of A_{2A}AR gene transfer on the regulation of NF-κB in HUVECs. A, confluent HUVECs were treated for 60 min in the absence of presence of 10 ng/ml TNFα before isolation of nuclei for incubation with a κB-selective oligonucleotide probe and the indicated antibodies for electrophoretic mobility shift assay analysis as described under *Materials and Methods*. The *asterisk* indicates a nonspecifically labeled band. This is one of multiple experiments. B, confluent HUVECs monolayers were infected at an m.o.i. of 25 pfu/cell with either a control GFP-encoding AV or AV/myc-human A_{2A}AR. After treatment with or without 10 ng/ml TNFα for the indicated times, soluble cell extracts were prepared and equalized for protein content before SDS-PAGE and immunoblotting with anti-IκBα antibody. This is one of multiple experiments. C, HUVECs plated onto glass coverslips were infected at an m.o.i. of 25 pfu/cell with either control AV/GFP or GFP AV/myc-human A_{2A}AR, which also expresses GFP from a separate open reading frame. After treatment with or without 10 ng/ml TNFα for 60 min as indicated, cells were fixed and permeabilized, and p65 was identified by staining with a p65-specific antibody and Alexa594-conjugated anti-rabbit IgG and by dual label confocal microscopy as described under *Materials and Methods*. HUVECs expressing recombinant protein are visible as *green* from GFP-derived fluorescence, whereas endogenous p65 is visible as *red*. This is one of multiple experiments.

mobilize intracellular calcium (Feoktistov and Biaggioni, 1997). This additional signaling capacity accounts for its reported ability to induce the expression of angiogenic factors from endothelial cells under conditions in which the A_{2A}AR does not (Feoktistov et al., 2002). Therefore, upon exposure to NECA, A_{2B}AR activation may counteract the simultaneous effects of A_{2A}AR activation under the same conditions, and this may explain why only CGS21680 reduces the adhesion observed at maximally effective concentrations of TNFα.

Some of the findings in HUVECs presented here are consistent with the recent observations of Majumdar and Aggarwal (2003), who described an adenosine-mediated inhibition of NF-κB in several cell types, including HeLa and cultured endothelial cells. Pharmacological analysis ruled out a contribution of A_1 and A_3ARs but did not address the specific involvement of A_{2A} or A_{2B}ARs in each of the cell types under investigation (Majumdar and Aggarwal, 2003). However, the data presented here would suggest that the A_{2A}AR subtype may be largely responsible for the inhibition of NF-κB observed by these investigators. A particularly important finding from Majumdar and Aggarwal (2003) was that adenosine specifically inhibited TNFα-induced NF-κB activation and nuclear translocation in the absence of any effect on IκB degradation, which is consistent with our observations in A_{2A}AR-expressing HUVECs. However, in contrast to their results, we found that A_{2A}AR expression blocked NF-κB–mediated induction of E-selectin by both TNFα and LPS, suggestive of an effect of the A_{2A}AR on the NF-κB nuclear translocation process that is common to both TNFR1 and TLR4 signaling cascades. This could be either reduced nuclear import of p50-p65 heterodimers and/or accelerated CRM1-mediated export of IκBα/NF-κB complexes out of the nucleus (Arenzana-Seisdedos et al., 1997).

A_{2A}AR activation elevates intracellular cAMP levels in HUVECs via interaction with G_s and stimulation of adenylyl cyclase (Klinger et al., 2002). Consistent with other investigators, we have noted that elevation of cAMP in endothelial cells is sufficient to ameliorate κB-dependent inflammatory responses, including adhesion molecule induction and subsequent monocyte adhesion (Morandini et al., 1996; W. A. Sands and T. M. Palmer, unpublished observations). However, the mechanisms by which this occurs seem to vary depending on the nature of the cAMP-elevating stimulus. For example, cyclic AMP-responsive element binding protein, which is phosphorylated on Ser^{133} and activated upon elevation of intracellular cyclic AMP levels, can directly block NF-κB-induced transcription without altering nuclear translocation or DNA binding by recruiting the transcriptional coactivator cAMP-responsive element binding protein-binding protein, thereby reducing the number of transcriptionally competent cAMP-responsive element binding protein-binding protein/NF-κB complexes (Parry and Mackman, 1997). In contrast, the cAMP-elevating hormone adiponectin inhibits NF-κB responses in ECs by inhibiting IKK-mediated IκB phosphorylation and degradation (Ouchi et al., 2000). The data from this study and that of Majumdar and Aggarwal (2003) argue that despite being able to elevate cAMP levels in HUVECs (Klinger et al., 2002), the A_{2A}AR inhibits NF-κB in these cells via a unique mechanism distinct from those employed by forskolin and adiponectin.

It should be noted, however, that despite the profound inhibitory effects of A_{2A}AR on NF-κB reported here, this is unlikely to be the only mechanism by which this receptor blocks inflammatory responses. A clue as to other potential mechanisms is suggested by our observation that although A_{2A}AR expression abolishes iNOS-mediated nitrite accumulation in response to LPS/TNFα/IFNγ treatment (Fig. 1), inhibition of NF-κB signaling by either PDTC pretreatment or expression of IκBα fails to completely block this effect (Fig. 5). Functional analysis of iNOS promoters in multiple species has revealed the presence of GAS sites, which bind activated signal transducer and activator of transcription 1 dimers, and interferon-regulatory factor-1 sites (Teng et al., 2002). Thus, complete inhibition of iNOS induction by the A_{2A}AR may also require inhibition of IFNγ signaling as well as NF-κB, an issue that we are currently addressing.

In conclusion, we have consolidated and extended previous studies investigating the anti-inflammatory effects of adenosine. In particular, we have demonstrated that increasing expression of the A_{2A}AR subtype suppresses NF-κB activation in two inflammatory cell types via distinct molecular mechanisms. The ability to specifically inhibit NF-κB activation via multiple routes is likely to be an important reason why the A_{2A}AR can exert its inhibitory effects even when cell type-specific mechanisms are in place to regulate NF-κB activation. In addition, the pronounced suppression of inflammatory responses seen upon A_{2A}AR gene transfer in our studies provides a complimentary counterpoint to the marked enhancement of inflammatory responses produced upon homozygous deletion of the A_{2A}AR in vivo and suggests that the A_{2A}AR acts as a rheostat whose expression controls cellular responsiveness to NF-κB-mobilizing stimuli. As such, our observations further underscore the importance of the A_{2A}AR as both a key target for generation of anti-inflammatory therapeutics for a wide range of disorders (Linden, 2001; Sitkovsky et al., 2004) and a protein whose defective regulation may influence the pathophysiology of diseases associated with either immune deficiency or suppression. Finally, the availability of model systems described herein that permit assessment of the anti-inflammatory signaling capacity of recombinant A_{2A}ARs in vitro can now allow a rigorous analysis of how changes in receptor phosphorylation and subcellular distribution in response to agonists or other stimuli (Palmer and Stiles, 1999; Burgueno et al., 2003) influence the magnitude and/or kinetics of the receptor's potent anti-inflammatory effects.

References

Arenzana-Seisdedos F, Turpin P, Rodriguez M, Thomas D, Hay RT, Virelizier JL, and Dargemont C (1997) Nuclear localization of IκBα promotes active transport of NF-κB from the nucleus to the cytoplasm. *J Cell Sci* **110:**369–378.

Armstrong JM, Chen JF, Schwarzschild MA, Apasov S, Smith PT, Caldwell C, Chen P, Figler H, Sullivan G, Fink S, et al. (2001) Gene dose effect reveals no G_s-coupled A_{2A} adenosine receptor reserve in murine T-lymphocytes: studies of cells from A_{2A}-receptor-gene-deficient mice. *Biochem J* **354:**123–130.

Banerjee SK, Young HW, Volmer JB, and Blackburn MR (2002) Gene expression profiling in inflammatory airway disease associated with elevated adenosine. *Am J Physiol* **282:**L169–L182.

Bouma MG, van den Wildenberg FA, and Buurman WA (1996) Adenosine inhibits cytokine release and expression of adhesion molecules by activated human endothelial cells. *Am J Physiol* **270:**C522–C529.

Brown GC and Bal-Price A (2003) Inflammatory neurodegeneration mediated by nitric oxide, glutamate and mitochondria. *Mol Neurobiol* **27:**325–355.

Burgueno J, Blake DJ, Benson MA, Tinsley CL, Esapa CT, Canela EI, Penela P, Mallol J, Mayor F Jr, Lluis C, et al. (2003) The adenosine A_{2A} receptor interacts with the actin-binding protein α-actinin. *J Biol Chem* **278:**37545–37552.

Cronstein BN, Montesinos MC, and Weissmann G (1999) Salicylates and sulfasalazine, but not glucocorticoids, inhibit leukocyte accumulation by an adenosine-dependent mechanism that is independent of inhibition of prostaglandin synthesis and p105 of NF-κB. *Proc Natl Acad Sci USA* **96:**6377–6381.

Dai Y, Rahmani M, and Grant S (2003) Proteasome inhibitors potentiate leukemic

cell apoptosis induced by the cyclin-dependent kinase inhibitor flavopiridol through a SAPK/JNK- and NF-κB-dependent process. *Oncogene* **22:**7108–7122.
Felsch A, Stocker K, and Borchard U (1995) Phorbol ester-stimulated adherence of neutrophils to endothelial cells is reduced by adenosine A_2 receptor agonists. *J Immunol* **155:**333–338.
Feoktistov I and Biaggioni I (1997) Adenosine A_{2B} receptors. *Pharmacol Rev* **49:**381–402.
Feoktistov I, Goldstein AE, Ryzhov S, Zeng D, Belardinelli L, Voyno-Yasenetskaya T, and Biaggioni I (2002) Differential expression of adenosine receptors in human endothelial cells: role of A_{2B} receptors in angiogenic factor regulation. *Circ Res* **90:**531–538.
Fredholm BB, IJzerman AP, Jacobson KA, Klotz KN, and Linden J (2001) International Union of Pharmacology XXV. Nomenclature and classification of adenosine receptors. *Pharmacol Rev* **53:**527–552.
He TC, Zhou S, da Costa LT, Yu J, Kinzler KW, and Vogelstein B (1998) A simplified system for generating recombinant adenoviruses. *Proc Natl Acad Sci USA* **95:**2509–2514.
Hevel JM and Marletta MA (1994) Nitric-oxide synthase assays. *Methods Enzymol* **233:**250–258.
Hirsch EC, Breidert T, Rousselet E, Hunot S, Hartmann A, and Michel PP (2003) The role of glial reaction and inflammation in Parkinson's disease. *Ann NY Acad Sci* **991:**214–228.
Jin X, Shepherd RK, Duling BR, and Linden J (1997) Inosine binds to A_3 adenosine receptors and stimulates mast cell degranulation. *J Clin Investig* **100:**2849–2857.
Karin M, Yamamoto Y, and Wang QM (2004) The IKK NF-κB system: a treasure trove for drug development. *Nat Rev Drug Discov* **3:**17–26.
Khoa ND, Montesinos MC, Reiss AB, Delano D, Awadallah N, and Cronstein BN (2001) Inflammatory cytokines regulate function and expression of adenosine A_{2A} receptors in human monocytic THP-1 cells. *J Immunol* **167:**4026–4032.
Klinger M, Kuhn M, Just H, Stefan E, Palmer T, Freissmuth M, and Nanoff C (2002) Removal of the carboxy terminus of the A_{2A}-adenosine receptor blunts constitutive activity: differential effect on cAMP accumulation and MAP kinase stimulation. *Naunyn Schmiedeberg's Arch Pharmacol* **366:**287–298.
Kobayashi S and Millhorn DE (1999) Stimulation of expression for the adenosine A_{2A} receptor gene by hypoxia in PC12 cells: a potential role in cell protection. *J Biol Chem* **274:**20358–20365.
Kumar S, Boehm J, and Lee JC (2003) p38 MAP kinases: key signalling molecules as therapeutic targets for inflammatory diseases. *Nat Rev Drug Discov* **2:**717–726.
Ledent C, Dumont JE, Vassart G, and Parmentier M (1992) Thyroid expression of an A_2 adenosine receptor transgene induces thyroid hyperplasia and hyperthyroidism. *EMBO (Eur Mol Biol Organ) J* **11:**537–542.
Ley K (2001) Pathways and bottlenecks in the web of inflammatory adhesion molecules and chemoattractants. *Immunol Res* **24:**87–95.
Linden J (2001) Molecular approach to adenosine receptors: receptor-mediated mechanisms of tissue protection. *Annu Rev Pharmacol Toxicol* **41:**775–787.
Majumdar S and Aggarwal BB (2003) Adenosine suppresses activation of nuclear factor-κB selectively induced by tumor necrosis factor in different cell types. *Oncogene* **22:**1206–1218.
Manning AM and Davis RJ (2003) Targeting JNK for therapeutic benefit: from junk to gold? *Nat Rev Drug Discov* **2:**554–565.
Monsonego A and Weiner HL (2003) Immunotherapeutic approaches to Alzheimer's disease. *Science (Wash DC)* **302:**834–838.
Montesinos MC, Yap JS, Desai A, Posadas I, McCrary CT and Cronstein BN (2000) Reversal of the antiinflammatory effects of methotrexate by the nonselective adenosine receptor antagonists theophylline and caffeine: evidence that the antiinflammatory effects of methotrexate are mediated *via* multiple adenosine receptors in rat adjuvant arthritis. *Arthritis Rheum* **43:**656–663.
Morandini R, Ghanem G, Portier-Lemarie A, Robaye B, Renaud A, and Boeynaems JM (1996) Action of cAMP on expression and release of adhesion molecules in human endothelial cells. *Am J Physiol* **270:**H807–H816.
Nguyen DK, Montesinos MC, Williams AJ, Kelly M, and Cronstein BN (2003) Th1 cytokines regulate adenosine receptors and their downstream signaling elements in human microvascular endothelial cells. *J Immunol* **171:**3991–3998.
Ohta A and Sitkovsky M (2001) Role of G-protein-coupled adenosine receptors in downregulation of inflammation and protection from tissue damage. *Nature (Lond)* **414:**916–920.
Oitzinger W, Hofer-Warbinek R, Schmid JA, Koshelnick Y, Binder BR, and de Martin R (2001) Adenovirus-mediated expression of a mutant IκB kinase 2 inhibits the response of endothelial cells to inflammatory stimuli. *Blood* **97:**1611–1617.
Ouchi N, Kihara S, Arita Y, Okamoto Y, Maeda K, Kuriyama H, Hotta K, Nishida M, Takahashi M, Muraguchi M, et al. (2000) Adiponectin, an adipocyte-derived plasma protein, inhibits endothelial NF-κB signaling through a cAMP-dependent pathway. *Circulation* **102:**1296–1301.
Palmer TM, Poucher SM, Jacobson KA, and Stiles GL (1995) ^{125}I-4-(2-[7-amino-2-[2-furyl][1,2,4]triazolo[2,3-*a*][1,3,5] triazin-5-yl-amino]ethyl)phenol, a high affinity antagonist radioligand selective for the A_{2A} adenosine receptor. *Mol Pharmacol* **48:**970–974.
Palmer TM and Stiles GL (1999) Stimulation of A_{2A} adenosine receptor phosphorylation by protein kinase C activation: evidence for regulation by multiple protein kinase C isoforms. *Biochemistry* **38:**14833–14842.
Parry GC and Mackman N (1997) Role of cyclic AMP response element-binding protein in cyclic AMP inhibition of NF-κB-mediated transcription. *J Immunol* **159:**5450–5456.
Read MA, Whitley MZ, Gupta S, Pierce JW, Best J, Davis RJ, and Collins T (1997) Tumor necrosis factor α-induced E-selectin expression is activated by the nuclear factor-κB and c-JUN N-terminal kinase/p38 mitogen-activated protein kinase pathways. *J Biol Chem* **272:**2753–27561.
Sexl V, Mancusi G, Holler C, Gloria-Maercker E, Schutz W, and Freissmuth M (1997) Stimulation of the mitogen-activated protein kinase *via* the A_{2A}-adenosine receptor in primary human endothelial cells. *J Biol Chem* **272:**5792–5799.
Sitkovsky MV, Lukashev D, Apasov S, Kojima H, Koshiba M, Caldwell C, Ohta A, and Thiel M (2004) Physiological control of immune response and inflammatory tissue damage by hypoxia-inducible factors and adenosine A_{2A} receptors. *Annu Rev Immunol* **22:**657–682.
Sun S, Elwood J, and Greene WC (1996) Both amino- and carboxyl-terminal sequences within IκBα regulate its inducible degradation. *Mol Cell Biol* **16:**1058–1065.
Taylor BS and Geller DA (2000) Molecular regulation of the human inducible nitric oxide synthase (iNOS) gene. *Shock* **13:**413–424.
Teng X, Zhang H, Snead C, and Catravas JD (2002) Molecular mechanisms of iNOS induction by IL-1β and IFN-γ in rat aortic smooth muscle cells. *Am J Physiol* **282:**C144–C152.
Wang CN, Shiao YJ, Lin YL, and Chen CF (1999) Nepalolide A inhibits the expression of inducible nitric oxide synthase by modulating the degradation of IκB-α and IκB-β in C6 glioma cells and rat primary astrocytes. *Br J Pharmacol* **128:**345–356.
Wyatt AW, Steinert JR, Wheeler-Jones CP, Morgan AJ, Sugden D, Pearson JD, Sobrevia L, and Mann GE (2002) Early activation of the p42/p44MAPK pathway mediates adenosine-induced nitric oxide production in human endothelial cells: a novel calcium-insensitive mechanism. *FASEB J* **12:**1584–1594.
Xie QW, Kashiwabara Y, and Nathan C (1994) Role of transcription factor NF-κB/Rel in induction of nitric oxide synthase. *J Biol Chem* **269:**4705–4708.

Address correspondence to: Dr. T. M. Palmer, 425 Davidson Bldg., University of Glasgow, Glasgow, G12 8QQ, UK. E-mail:t.palmer@bio.gla.ac.uk